JOURNAL OF ELECTROMAGNETIC ENGINEERING AND SCIENCE, VOL. 22, NO. 2, 162~170, MAR. 2022

https://doi.org/10.26866/jees.2022.2.r.73
ISSN 2671-7263 (Online) · ISSN 2671-7255 (Print)

# Analytical Modeling of Self- and Mutual Inductances of DD Coils in Wireless Power Transfer Applications

Ali Alkasir[1] · Seyed Ehsan Abdollahi[1,*] · Seyedreza Abdollahi[2] · Patrick Wheeler[3]

## Abstract

Self- and mutual inductances are major design parameters for wireless power transfer (WPT) systems. To optimize a WPT system and estimate its performance in terms of received power and efficiency, it is essential to obtain a simple, fast, and accurate calculation of these two parameters. The polarized double-D (DD) coils were selected due to their simplicity of structure, high efficiency, and low sensitivity to misalignment conditions. This paper presents analytical calculations of self- and mutual inductance using the Biot-Savart law for DD coils. The results of the analytical calculations of mutual inductance in different distances between coils were investigated, and the results of the calculations were verified using experimental and finite element method (FEM) simulation results. This paper also presents analytical and FEM-based optimization guidelines for the coupling coefficient of the transmitter coil.

**Key Words**: Analytical Modeling, Mutual Inductance, Polarized DD Coils, Self-inductance, Wireless Power Transfer.

## I. Introduction

Wireless power transfer (WPT) technology has attracted considerable attention in recent years due to its ease of use, high reliability, safety, and automatic accessibility to electrical power [1]. WPT can be used in applications such as medical implants [2], robotics [3], and electronic devices [4]. Given the above-mentioned benefits, the WPT system may be an appropriate alternative to wired charging systems in electric vehicles.

The static wireless charging (SWC) system has the above advantages, while the dynamic wireless charging (DWC) system, in addition to the above advantages, provides solutions to increase the range of motion, reduce size of lithium-ion battery, and eliminate waiting time for charging an electric vehicle [1].

WPT systems have two coils, one acting as the transmitter coil and the other as the receiver coil. Coils can be implemented in solenoid or spiral forms. Spiral coils occupy less space (volume) than solenoid coils. Also, these coils, wound in a spiral form with increasing radius, have a much better coupling coefficient than a solenoid coil wound around a fixed radius. As shown in Fig. 1, the WPT coils were categorized into polarized and non-polarized groups. Non-polarized coils have one pole on the transmitter side and one opposite pole on the receiver side, while polarized coils have two opposite poles on the transmitter side and two opposite poles on the receiver side. The height of the flux path ($h_2$) in polarized coils is significantly higher than non-polarized coils ($h_1$) for a similar size. As a result, the coupling coefficient is higher in the polarized coils and is also more robust to misalignment in the horizontal direction [1], which makes the coils more appropriate for their application in electric

Manuscript received January 29, 2021 ; Revised May 7, 2021 ; Accepted July 18, 2021. (ID No. 20210129-021J)
[1]Department of Electrical and Computer Engineering, Babol Noshirvani University of Technology, Babol, Iran.
[2]Department of Electrical and Computer Engineering, University of Science and Technology of Mazandaran, Behshahr, Iran.
[3]Department of Electrical and Electronic Engineering, University of Nottingham, Nottingham, UK.
[*]Corresponding Author: Seyed Ehsan Abdollahi (e-mail: e.abdollahi@nit.ac.ir)

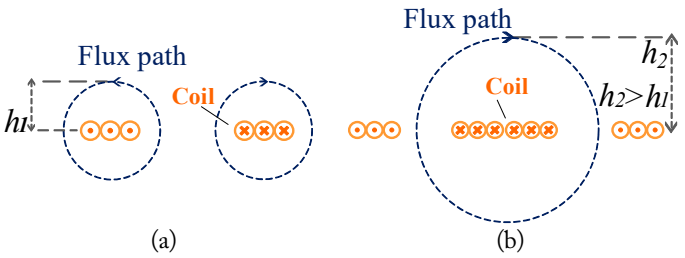


Fig. 1. Spiral WPT coils: (a) non-polarized coil and (b) polarized coil.

vehicle charging in both SWC and DWC methods. Among polarized coils, the double-D (DD) design is preferred due to its simple structure, high efficiency, and low sensitivity in misalignment conditions [5]. To optimize a WPT system or estimate its operating parameters (such as received power, efficiency, and gain), the designer should accurately compute the self- and mutual inductances [6]. These computations could be carried out using analytical, numerical (finite element method [FEM]) [7], or hybrid analytical-numerical methods. The analytical method has remarkable advantages over the other methods due to its time-saving analysis and cost effectiveness. Though many studies have been carried out to compute self- and mutual inductances of WPT system coils for circular [8–11] and square structures [12–14], few studies have been published regarding rectangular [15, 16] and DD power coils [17]. An analytical method to compute self- and mutual inductances of spiral rectangular coils is presented in [18]. However, it is rather complicated due to its dependence on computers and the need to set initial burdensome values [6]. A numerical-analytical method based on infinite integral, infinite Bessel series, and trigonometric functions is proposed in [19] to calculate the mutual inductance between two rectangular coils, which must be resolved numerically [20]. An analytical method to calculate inductance for multi-loop spiral coils is proposed in [21] based on Grover equations [22], which for each piece of conductor, the self- and mutual inductances must be computed and added together. Applying this method to compute the inductance of multi-loop coils is time-consuming, even with fast computers [16]. In [17], the Grover-based method is used to calculate self-inductance, and the Neumann-based method is employed for mutual inductance. This method is not ideal for the computation of DD power coils in terms of computational errors. Also, since no experimental setup has been implemented, the analytical results were not validated by any experimental results.

This paper obtains self- and mutual inductances of transmitter and receiver's DD coils by analytically employing the Biot-Savart law, which is simpler than the abovementioned methods. For demonstration, we validated the analytical calculations using the numerical and measurement results. We also obtained the mutual inductances for various DD coil distances (coaxial) using the proposed analytical method, as well as numerical and experimental methods. According to the low error between spiral and single-loop coil inductances in the proposed method, each spiral multi-turn coil is considered a several-filament single-loop coil. Finally, we examine the optimized dimensions of the transmitter's coil in terms of the coupling coefficient across the coils on the condition that the dimension of the receiver's coil is constant.

## II. Analytical Modeling of DD Coils

### 1. Computation of Self-inductance

Fig. 2(a) shows a DD coil, which consists of two D-shaped spiral sub-coils and, in series form, electrically. According to Fig. 2(b) and 2(c), for simplification purposes, each spiral sub-coil is considered a several-concentric single-loop coil. According to Fig. 2(c), $w$ is the wire diameter and $s$ is the distance between two adjacent wires. Variables in Fig. 2(d), including the length and width of the loops, are $a$, $b$. The dimensions of the $i^{th}$ loop, including $a_i$ and $b_i$ can be obtained by

$$a_i = a_1 - (i-1)(2w+2s),\ b_i = b_1 - (i-1)(2w+2s), \tag{1}$$

where $i = 1$ is the outermost loop.

To obtain the self-inductance of a loop, the flux enclosed by that loop must be computed and divided into the loop current. The flux of $i^{th}$ loop is obtained according to

$$\Phi_i = \int_{S_i} B_i \,.\, dS_i = \int_{S_i} B_i \, dS_i, \tag{2}$$

where $B_i$ is the field density, and $S_i$ is the cross-section of $i^{th}$ loop. According to right-hand law, the field density is perpendicular to the plane. Therefore, given the perpendicularity of the unit vector on the $yz$ plane, according to Fig. 2(c), the internal multiplication is eliminated. Moreover, since, in this case, the largest physical dimension of coil a, relative to wavelength λ, is electrically very small (i.e., $a \ll \lambda$), the frequency effect of the source could be neglected [23]. Hence, Eq. (2) can be used to compute the self- and mutual inductances.

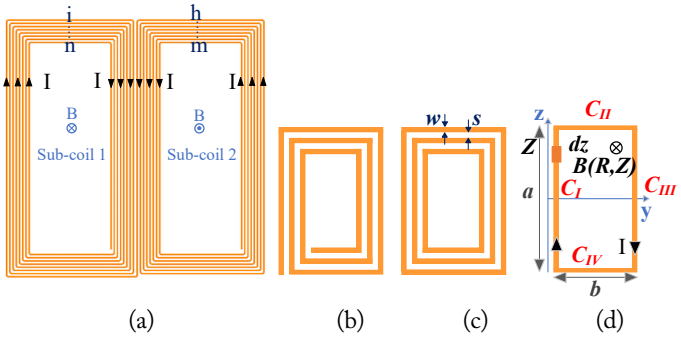


Fig. 2. (a) DD coil. (b) Spiral sub-coil. (c) A set of concentric loops. (d) A rectangular loop.

The flux density of conductor $C_I$, in Fig. 2(d), is obtained using the Biot-Savart law according to (3). In the following, Eqs. (3)–(6) are applied to calculate the flux density and flux caused by conductor $C_I$, as well as the total flux of the loop, respectively [24].

$$B_{C_I} = \frac{\mu_0 I}{4\pi R}\left[\frac{Z+\frac{a}{2}}{\sqrt{\left(Z+\frac{a}{2}\right)^2+R^2}} - \frac{Z-\frac{a}{2}}{\sqrt{\left(Z-\frac{a}{2}\right)^2+R^2}}\right]. \tag{3}$$

$R$ is the distance between the element and the point at which we are computing the magnetic field $B$, which can be defined as

$$R = \sqrt{(Z-\frac{a}{2})^2 + r^2}, \tag{4}$$

where $Z$ is the distance of the given point to the $xy$ plane, $r$ is the perpendicular distance of the given point to the $z$ axis, $\mu_0$ is the vacuum permeability coefficient, and $I$ is the loop current, the value of which is considered a unit. Loop flux, caused by $C_I$ conductor current in Fig. 2(c), is computed by

$$\Phi_{C_I-i} = \int_{Z=\frac{w}{2}-\frac{a}{2}}^{\frac{a}{2}-\frac{w}{2}} \int_{R=\frac{w}{2}}^{b-\frac{w}{2}} B_{cI}\, dR dZ. \tag{5}$$

To obtain the total flux of the loop (conductors $C_I$, $C_{II}$, $C_{III}$, $C_{IV}$), flux caused by all four conductors should be added. Thus, the total flux of loop $i$ caused by the current of the loop itself, is as follows:

$$L_i = \Phi_{i-i} = 2\int_{Z=\frac{w}{2}-\frac{a}{2}}^{\frac{a}{2}-\frac{w}{2}} \int_{R=\frac{w}{2}}^{b-\frac{w}{2}} Bc_I dR dZ + 2\int_{Z=\frac{w}{2}-\frac{b}{2}}^{\frac{b}{2}-\frac{w}{2}} \int_{R=\frac{w}{2}}^{b-\frac{w}{2}} Bc_{II} dR dZ =$$
$$2\frac{\Phi_I+\Phi_{II}}{I} = \frac{\mu_0}{\pi}\left(-a\ln\left(1+\sqrt{1+\left(\frac{b}{a}\right)^2}\right) - b\ln\left(1+\sqrt{1+\left(\frac{a}{b}\right)^2}\right) + a\ln\frac{2b}{\frac{w}{2}} + b\ln\frac{2a}{\frac{w}{2}} + 2\sqrt{a^2+b^2} - 2b - 2a\right). \tag{6}$$
$$a, b \gg \frac{w}{2}$$

In Eq. (6), inductance is obtained by assuming $a, b \gg \frac{w}{2}$. Also, due to the ineffectiveness of the current in the inductance value, its value is considered a unit, hence, $\Phi_{i-i} = L_i$. In the following self-inductance computation of DD coils, the mutual inductance of the loops of sub-coil 1 together, the mutual inductance of the loops of sub-coil 2 together, and the mutual inductance between the loops of sub-coils 1 and 2 together should be obtained and added. Given that the coils of WPT systems are wound with Litz wire and normally operate at a working frequency of less than 100 kHz, the skin effect is negligible. Consequently, the filamentary is logical for the Litz wire [14]. Fig. 3 shows loop $i$ as part of sub-coil 1 through which current $I_1$ flows, and the objective is to compute mutual inductance in loop $j$ or $h$. According to the DD coil structure, if the other loop is part of sub-coil 2 (loop $h$), it would be on the right side of loop $i$ (right-side dashed-line loop), in which case $S_a$ is negative and $S_b$ is positive. If the other loop (loop $j$) is part of sub-coil 1, it would be inside loop $i$ (in-loop $i$ dashed-line loop), in which case $S_a$ and $S_b$ are negative.

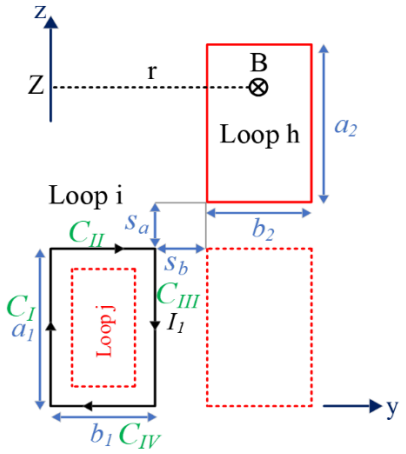


Fig. 3. Computation of mutual flux between two loops from one sub-coil or between two loops from two sub-coils of a DD coil.

To calculate the mutual inductance of loops $h$ or $j$, the flux enclosed to loops $h$ or $j$ should be divided on current $I_1$ (as part of loop $i$):

$$M_{i-j,h} = \frac{\Phi_{i-j,h}}{I_1}, \tag{7}$$

where $\Phi_{i-j,h}$ is the enclosed flux to loops $h$ or $j$, and $I_1$ is the current of loop $i$. The enclosed flux to loops $h$ or $j$ is obtained according to the following equation:

$$\Phi_{i-j,h} = \int_{S_{j,h}} B_{i-j,h}.dS_{j,h} = \int_{S_2} B_{i-j,h} ds_{j,h}, \tag{8}$$

where $S_{j,h}$ is the plane of loop $j$ or $h$, and $B_{i-j,h}$ is the field density. According to the right-hand law, the field density is perpendicular to the plane. As a result, internal multiplication could be eliminated. The formula for field density is obtained through the Biot-Savart law, which is similar to Eq. (3). The difference is that it is shifted toward the positive part of the $z$-axis (Fig. 3) as much as $\frac{a}{2}$. The magnetic flux of loops $h$ or $j$, caused by the current of conductor $C_I$, is brought below. In the following, Eqs. (9) and (10) are applied to compute the flux of loops $h$ or $j$, caused by the current of conductor $C_I$ and loop $i$ [24].

$$\Phi_{C_I-j,h} = \frac{\mu_0 I}{4\pi}\int_{r=r_1}^{r_2}\int_{Z=Z_1}^{Z_2}\frac{1}{r}\left[\frac{Z}{\sqrt{Z^2+r^2}} - \frac{Z-a}{\sqrt{(Z-a)^2+r^2}}\right] dZ dr = \frac{\mu_0 I}{4\pi}\left[\sqrt{Z_2^2+r_2^2} - Z_2\ln\left(Z_2+\sqrt{Z_2^2+r_2^2}\right) - \sqrt{Z_2^2+r_1^2} + Z_2\ln\left(Z_2+\sqrt{Z_2^2+r_1^2}\right) - \sqrt{Z_1^2+r_2^2} + Z_1\ln\left(Z_1+\sqrt{Z_1^2+r_2^2}\right) + \sqrt{Z_1^2+r_1^2} - Z_1\ln\left(Z_1+\sqrt{Z_1^2+r_1^2}\right) - \sqrt{(Z_2-a_1)^2+r_2^2} + \left((Z_2-a_1)\ln((Z_2-a_1)+\sqrt{(Z_2-a_1)^2+r_2^2}\right) + \sqrt{(Z_2-a_1)^2+r_1^2} - (Z_2-a_1)\ln\left((Z_2-a_1)+\sqrt{(Z_2-a_1)^2+r_1^2}\right) + \sqrt{(Z_1-a_1)^2+r_2^2} - (Z_1-a_1)\right].$$
$$Z_1 = a_1 + s_a,\ Z_2 = a_1 + s_a + a_2,\ r_1 = b_1 + s_b,\ r_2 = b_1 + s_b + b_2 \tag{9a}$$

The above equation can be further compressed as

$$\Phi_{C_I-j,h} = \frac{\mu_0 I}{4\pi} K(Z_1, Z_2, r_1, r_2, a_1). \quad (9b)$$

According to the right-hand law, conductors $C_I$ and $C_{IV}$ create imported flux, and conductors $C_{II}$ and $C_{III}$ create exported flux on the plane of loops $h$ or $j$. Therefore, the mutual inductance equation per four inductors is as follows:

$$M_{i-j,h} = \frac{\mu_0}{4\pi} K(a_1 + s_a, a_1 + s_a + a_2, b_1 + s_b, b_1 + s_b + b_2, a_1) - K(a_1 + s_a, a_1 + s_a + a_2, s_b, s_b + b_2, a_1) - K(b_1 + s_b, b_1 + s_b + b_2, s_a, s_a + a_2, b_1) + K(b_1 + s_b, b_1 + s_b + b_2, a_1 + s_a, a_1 + s_a + a_2, b_1). \quad (10)$$

Sub-coils 1 and 2 are similar; thus, by doubling $L_{sc1}$, inductance of a DD coil is obtained and is represented by $L_{DD}$.

$L_{DD}$ self-inductance of a DD coil is analytically obtained as

$$L_{DD} = 2 * \left(\sum_{i=1}^{n} L_{sc1(i)} + \sum_{i=1}^{n}\sum_{j=1}^{n} M_{sc1(i,j)}(i \neq j) + \sum_{i=1}^{n}\sum_{h=1}^{m} M_{sc1,2(i,h)}\right), \quad (11a)$$

where $L_{sc1}$, $M_{sc1}$, and $M_{sc1,2}$ are the self-inductance of sub-coil 1, the mutual inductance between loops of sub-coil 1, and the mutual inductance between loops of sub-coils 1 and 2. Using the results of Section IV, it can be inferred that section $M_{sc1,2}$ of self-inductance calculations can be neglected due to its low effect on the intended response and to reduce the complexity of the calculations. Therefore, Eq. (11a) can be simplified as follows:

$$L_{DD} = 2 * \left(\sum_{i=1}^{n} L_{sc1(i)} + \sum_{i=1}^{n}\sum_{j=1}^{n} M_{sc1(i,j)}(i \neq j)\right). \quad (11b)$$

This formula holds true when ferromagnetic materials are not used. The proposed model can be easily developed for this case by inserting a scaling factor for $\mu_r$ in Eqs. (6) and (10) [9, 13].

The flowchart in Fig. 4 demonstrates how the self-inductance of the transmitter and receiver coils is calculated. As observed in the flowchart, $i$, $j$, and $n$ are symbols of loop numbers of sub-coil 1. The sum of the self-inductance of sub-coil 1 is named sum 1, and the mutual inductance between loops of sub-coil 1 is named sum 2. The total sum of sum 1 and sum 2 composes the self-inductance of sub-coil 1 and is presented by $L_{sc1}$ in the relevant flowchart. Sub-coils 1 and 2 are similar; thus, by doubling $L_{sc1}$, the inductance of a DD coil is obtained and is represented by $L_{DD}$.

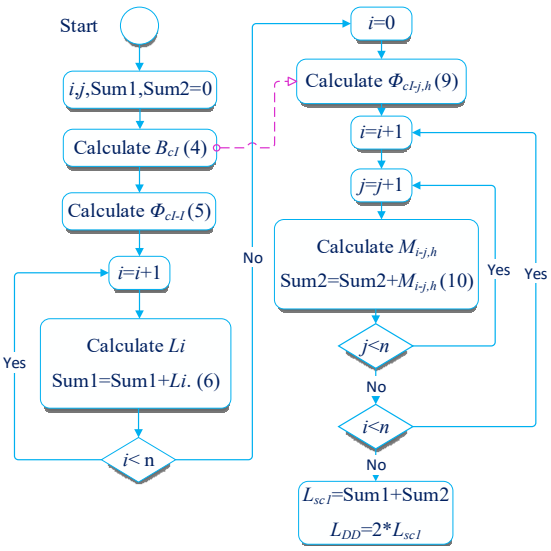


Fig. 4. Computation of self-inductance of DD coil.

*2. Computation of Mutual Inductance*

The DD coils of the transmitter and receiver are shown in Fig. 5(a). Given the above explanation in Section II-1, DD coils consist of a Litz conductor. Moreover, since the operating frequency of these systems is normally less than 100 kHz, the skin effect is negligible here and filamentary is logical. Also, each sub-coil is considered a several-concentric filamentary single-loop. The outer loops of sub-coils 1 and 3 of DD coils are shown in Fig. 5(b). The formula of mutual inductance for DD coils is then computed by

$$M_{DD} = M_{sc1,3} + M_{sc2,4} + M_{sc1,4} + M_{sc2,3}, \quad (12)$$

where $M_{sc1,3}$, $M_{sc2,4}$, and $M_{sc1,4}$, $M_{sc2,3}$ are mutual inductances of the facing sub-coils and mutual inductances of non-facing sub-coils in DD coils, respectively. According to the investigation presented in Section IV, since the mutual inductance value is insignificant in non-facing sub-coils, they are neglected to avoid computational complications. Hence, Eq. (12) is simplified as

$$M_{DD} = M_{sc1,3} + M_{sc2,4}. \quad (13)$$

The mutual inductance between $i^{th}$ single-loop (transmitter) and $u^{th}$ single-loop (receiver), according to Fig. 5(b), is obtained from the division of flux of $u^{th}$ loop to the current of $i^{th}$ loop as

$$M_{iu} = \frac{\Phi_{iu}}{I_i}. \quad (14)$$

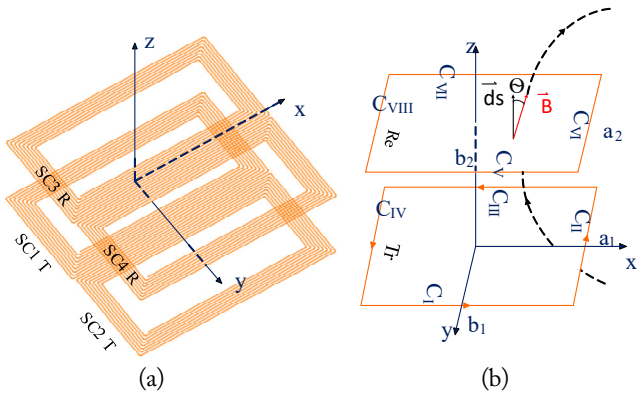


Fig. 5. (a) Set of DD coils. (b) Two filament loops of the transmitter and receiver coils.

Then, the flux of $u^{th}$ loop is calculated from

$$\Phi_{iu} = \int_{S_u} B_{iu} \,.\, dS_u = \int_{S_u} B_{iu}\, dS_u\, cos\Theta. \tag{15}$$

$B_{iu}$ is the field density caused by the conductor $C_{II}$, and $S_u$ is the plane of $u^{th}$ loop. Also, the point here represents internal multiplication. $\Theta$ is the angle between the unit vector of the plane of $u^{th}$ loop and the vector of $B_{iu}$ field density (Fig. 5(b)). According to the Biot-Savart law, the equation of field density along the $z$-axis is as below. Eqs. (16) and (17) are the flux density and flux (or mutual inductance) of conductor $C_{II}$ [20].

$$B_{C_{II}-z} = \frac{\mu_0 I}{4\pi} \frac{\frac{b}{2}-y}{\left(\frac{b}{2}-y\right)^2+z^2} \left[ \frac{\frac{a}{2}+x}{\sqrt{\left(\frac{b}{2}-y\right)^2+z^2+\left(\frac{a}{2}+x\right)^2}} + \frac{\frac{a}{2}-x}{\sqrt{\left(\frac{b}{2}-y\right)^2+z^2+\left(\frac{a}{2}-x\right)^2}} \right]. \tag{16}$$

Also, magnetic flux caused by conductor $C_{II}$ along the $z$-axis, which is the effective component for computing mutual flux, is obtained by

$$\begin{aligned}\Phi_{C_{II}-z} = \int_{-\frac{b_2}{2}}^{\frac{b_2}{2}} dy \int_{-\frac{c_2}{2}}^{\frac{c_2}{2}} B_{C_I-z} dx = \frac{\mu_0 I}{4\pi} \Big[ &\sqrt{(b_1+b_2)^2+z^2+(a_1+a_2)^2} - \\ (a_1+a_2).tanh^{-1} &\frac{a_1+a_2}{\sqrt{(b_1+b_2)^2+z^2+(a_1+a_2)^2}} - \sqrt{(b_1+b_2)^2+z^2+(a_1-a_2)^2} + \\ (a_1+a_2).tanh^{-1} &\frac{a_1-a_2}{\sqrt{(b_1+b_2)^2+z^2+(a_1-a_2)^2}} - \sqrt{(b_1-b_2)^2+z^2+(a_1+a_2)^2} + \\ (a_1+a_2).tanh^{-1} &\frac{a_1+a_2}{\sqrt{(b_1-b_2)^2+z^2+(a_1+a_2)^2}} + \sqrt{(b_1-b_2)^2+z^2+(a_1-a_2)^2} - \\ (a_1-a_2).tanh^{-1} &\frac{a_1-a_2}{\sqrt{(b_1-b_2)^2+z^2+(a_1-a_2)^2}} \Big].\end{aligned} \tag{17}$$

According to Fig. 5(b), $a_1$, $b_1$, $a_2$, and $b_2$ are the dimensions of the transmitter's and receiver's loops, and $z$ is the distance between two loops along the $z$-axis. Given the conductors' symmetry, $\Phi_{C_I} = \Phi_{C_{III}}$ and $\Phi_{C_{II}} = \Phi_{C_{IV}}$ are equal. To obtain the magnetic field of the conductor $\Phi_{C_{II}}$ in Eq. (17), $a_1$ and $a_2$ should be replaced with $b_1$ with $b_2$, respectively. According to right-hand law, the general formula of the magnetic field is equal to $\Phi_{iu} = \Phi_{C_I} + \Phi_{C_{II}} + \Phi_{C_{III}} + \Phi_{C_{IV}}$. The general mutual inductance is obtained as

$$M_{DD} = M_{sc1,3} + M_{sc2,4} = \sum_{i=1}^{n}\sum_{u=1}^{v} M_{iu} + \sum_{h=1}^{m}\sum_{w=1}^{x} M_{hw}, \tag{18}$$

where $i$ and $n$ are loops of sub-coil 1; $h$ and $m$ are loops of sub-coil 2; $u$ and $v$ are loops of sub-coil 3; and $w$ and $x$ are loops of sub-coil 4. This formula holds true when ferromagnetic materials are not used. The proposed model can be easily developed for this case by inserting a scaling factor for $\mu_r$ in Eqs. (18) [9, 13].

## III. Finite Element Modelling of DD Coils

The FEM model was developed in Altair Flux3D to confirm the proposed analytical model and obtain the magnetic parameters of $L_{DDT}$, $L_{DDR}$, $M$, and $k$. The model is designed based on the parameters given in Table 1.

Table 1. Geometrical and electrical parameters of DD coils

| Item | Value |
|---|---|
| Sub-coil dimension | 400 × 200 mm |
| DD coil dimension | 400 × 400 mm |
| $N_{sc1}$, $N_{sc2}$ | |
| Transmitter | 11, 11 turn |
| Receiver | 6, 6 turn |
| $w$, $s$ | 3, 3 mm |
| Airgap | 10–100 mm |
| System operating frequency | 85.5 kHz |
| $R_1$, $R_2$ | 0.038 Ω, 0.096 Ω |
| Litz wire | 400 × 0.1 mm |

Fig. 6(a) shows the 3D-FEM model of DD coils, and Fig. 6(b) represents the coil's magnetic flux path. According to Fig. 6(a), in the FEM simulation, each transmitter and receiver consists of two sub-coils. Each sub-coil consists of 11 transmitter coil and 6 receiver coil separate conductor loops. After building the transmitter separate loops in the FEM simulation, all the transmitter loops are assigned to one coil (transmitter coil); therefore, all the loops are electrically in series. The same is true for the receiver coil. The coils in the FEM simulation are like the prototypes considered in the analytical model as well as the experimental prototype; however, the difference is that the analytical case does not have rounded corners, and FEM and analytical simulations, compared to the experimental prototype of DD coils, are considered separate loops instead of spirals. Using the FEM simulation, the coils were modeled into spirals and separate loops, and the errors for $L_{DDT}$, $L_{DDR}$, and $M$, are 0.25%, 0.5%, and 0.77%, respectively.

### *1. Coupling Coefficient Optimization*

In some applications of the WPT system, such as medical

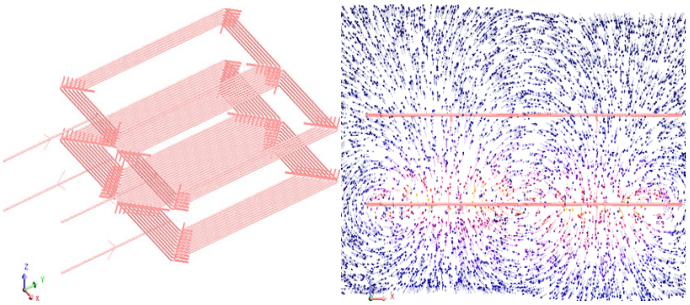

(a) (b)

Fig. 6. A 3D-FEM model: (a) DD coils and (b) vector schematic of the magnetic flux density.

implants, cell phones, and robotics (UAV), the receiver coil has some limitations in terms of dimensions and weight. In electric vehicle applications, the receiver coil has a definite and specified size according to the SAE J2954A standard [37]; however, the transmitter coil normally does not have any restrictions in dimension and weight. Hence, by changing the dimensions of the transmitter coil, the coupling coefficient and efficiency can be improved. Given the intended approximations for calculating self- and mutual inductances in this paper, a DD coil might be composed of several rectangular loops. The effect of the dimension change of a loop from the transmitter loop relative to constant receiver loop dimensions on the coupling coefficient is investigated using the analytical and FEM methods shown in Fig. 7.

According to the results in Fig. 7, the highest coupling coefficient occurs at a distance of $10 < z < 100$ mm between the transmitter and receiver loops in the case that they are similar (400 × 200 mm). From a $100 < z < 150$ mm distance between loops, a transmitter loop with a dimension of 500 × 250 mm creates the highest $k$. Also, at a distance of $z > 150$ mm, the transmitter loop with 600 × 300 mm dimensions has the highest $k$.

Consequently, according to the results in Fig. 7, in low distances between the two loops, equal dimensions of the transmitter and receiver loops result in an optimal state. By increasing the distance between loops and the dimensions of the transmitter loop, the optimal coupling coefficient is achieved.

## IV. Experimental Results and Coupling Coefficient Optimization

### 1. Self-inductance Measurement

An experimental setup was implemented to investigate the accuracy of the analytical method for obtaining the self- and mutual inductances of DD coils (Fig. 8). Table 1 presents the specifications of the coils. In this research, the RLC meter, Lutron LCR-9184 model (Lutron Electronic Enterprise Co. Ltd., Taipei, Taiwan) is employed to measure self- and mutual inductances of DD coils.

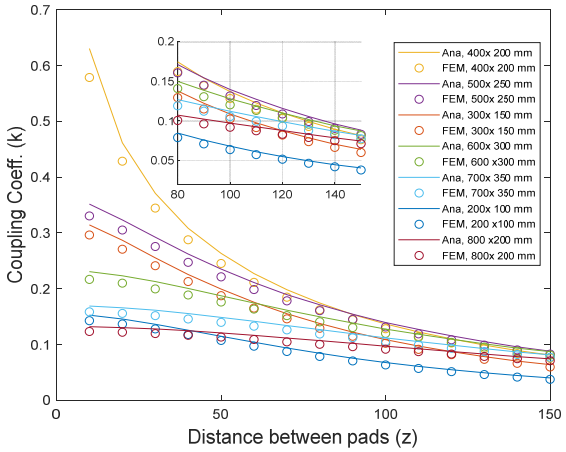


Fig. 7. A comparison of the coupling coefficient of a loop from the transmitter and receiver coils and the distance change between the two loops while the dimension of the transmitter loop is variable. The solid and circular curves are the results of the analytical calculations and FEM, respectively.

Fig. 9 shows the results of the self-inductance of the transmitter's and receiver's DD coils when applying the analytical, FEM, and experimental methods. From the results shown in Fig. 9(a), comparing the numbers obtained for self-inductance through the abovementioned methods (without approximating the elimination of the mutual inductance between two sub-coils of a coil $M_{sc1,2}$ or $M_{sc3,4}$) proves that the occurred errors are very small, such that the maximum result error is 4.38% (Fig. 9(b)). According to the analytical results marked by a star in Fig. 9, it could be observed that by neglecting mutual inductance between sub-coils 1 and 2 in the transmitter coil ($M_{sc1,2}$) or between sub-coils 3 and 4 in the receiver coil ($M_{sc3,4}$) for the self-inductance calculation (for simplification), the maximum error between the analytical-experimental results is 6.08% and between the analytical-simulation is 7.93%, which is acceptable.

To show the performance of the proposed method, we com-

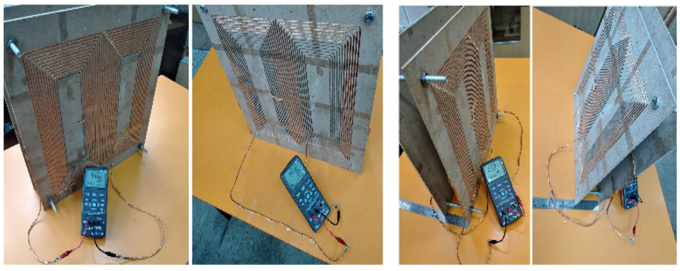

(a) (b)

Fig. 8. Measuring inductance of DD coils: (a) self-inductance and (b) mutual inductance.

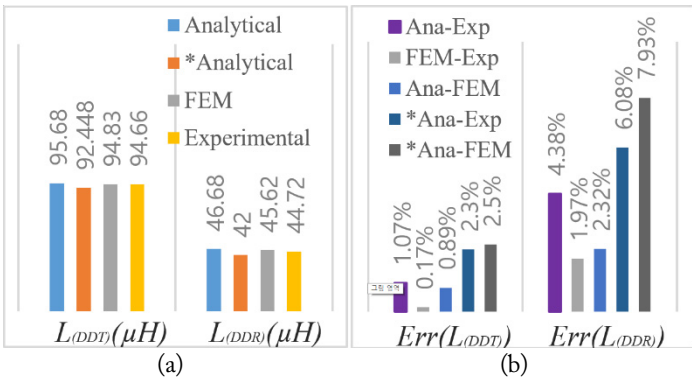


(a) (b)

Fig. 9. Comparison calculation of the measured and simulated self-inductance of the transmitter and receiver DD coils: (a) self-inductances and (b) errors in the results. $M_{sc1,2}$ and $M_{sc2,4}$ are not considered in the analytical results that are marked by star (*).

pared the self-inductance of a loop of one sub-coil and one loop of a DD coil with the findings in [17]. As shown, the results of FEM-EXP and ANA-EXP in the proposed method for a single loop of a sub-coil and DD coil are significantly better than those of [17].

To investigate the accuracy of the formula and approximations for obtaining mutual inductance between DD coils, we developed the experimental prototype shown in Fig. 8(b), which uses an RLC meter connection to obtain $M_{DD}$. To measure mutual inductance, one can act as shown in Fig. 8(b).

Fig. 10(a) shows the computation results of the mutual inductance between the transmitter and receiver DD coils with a distance of 10–100 mm between the two coils, obtained using the analytical, experimental, and FEM simulation methods. As shown in Fig. 10(b), the maximum error of the mutual inductance between the two coils in the analytical-experimental, simulation-experimental, and analytical-simulation methods are 9.12%, 8.68%, and 9.16%, respectively, which occurs in very small air gap between the two coils. As the distance between the transmitter and receiver coil increases, the chance of computational error reduces, such that with a 100-mm distance between two coils, the error values for the analytical-experimental, simulation-experimental, and analytical-simulation methods are 0.54%, 0.54%, and 1.06%, respectively. The error value observed in the results of mutual inductance $M_{DD}$ is caused by an approximation of the neglected mutual inductance in non-facing sub-coils, error measurement, and errors caused by considering a spiral coil in several concentric filamentary single-loop forms.

*2. Comparison of the Simulation and Proposed Analytical Model*

Table 2 shows a comparison of the computation times for the Altair Flux3D and the proposed analytical model (MATLAB) to obtain self- and mutual inductances. The simulations were executed on an Intel Core i7-7500U CPU with a processor 2.7 GHz clock speed and 12 GB RAM (Asus K541U). The comparison confirms that the use of the proposed analytical model saves significant computational time.

Also, by disregarding $M_{sc1,2}$ and $M_{sc3,4}$, the number of iterations of the equations (calculate $L_{DDT}$) will decrease from 484 to 242; as a result, the computation time will be reduced to 0.13 seconds.

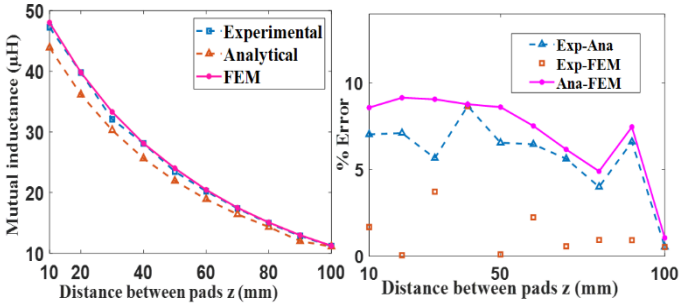


(a) (b)

Fig. 10. Mutual inductance relative to distance change between the two coils. (a) A comparison of the results of mutual inductance obtained from the analytical, experimental, and FEM methods. (b) A comparison of the error results.

Table 2. Comparison of the simulation and proposed analytical model

| Configuration of the coils | Simulation time | |
|---|---|---|
| | 3D FEM | Proposed |
| $L_{SC}$ (single loop) | 3 min | $52 \times 10^{-3}$ s |
| $L_{DDT}$ (total loops) | 6 min | 0.5 s |
| $M_{sc1,3}$ (single loops) | 3 min | $20 \times 10^{-3}$ s |
| $M_{DD}$ (total loops) | 9 min | 0.4 s |
| $M_{DD}$ (single loop, 0–100 mm distance between coils) | 34 min | $20 \times 10^{-3}$ s |
| Optimization $k$ (Fig. 7) | 2 h 5 min | 0.1 s |

## V. CONCLUSION

This paper presented an analytical computational method for the self-inductance of two DD coils and mutual inductance. Analytical computations, FEM, and experimental results of self- and mutual inductances were obtained and compared. The proposed method is simpler than existing methods. The findings showed that the elimination of $M_{sc1,2}$ and $M_{sc3,4}$ in the calculation of self-inductances and $M_{sc1,4}$ and $M_{sc2,3}$ in the mutual inductance calculation reduces the complexity of analytical calculations but does not considerably affect the proposed method accuracy. The optimization of the coupling coefficient on the transmitter coil was performed in applications where the receiver coil had a size or weight limit. Table 3 also proves the accuracy of the results of the proposed method compared to the existing literature. An analytical model could be applied to design and optimize the DD coils of a WPT system; nonetheless,

Table 3. Comparison of [17] and the proposed method

| Coil description | Dashora et al. [17] | | Proposed | |
|---|---|---|---|---|
| | $L_{SC}$ | $L_{SC}$ | $L_{SC}$ | $L_{DD}$ |
| Ana (μH) | 0.8 | 1.9 | 1.06 | 2.23 |
| Fem (μH) | 0.74 | 1.74 | 1.03 | 2.44 |
| Exp (μH) | - | - | 1.06 | 2.38 |
| $E_{rr}$ (%) | | | | |
| Fem-Exp | 30 | 27 | 1.70 | 2.50 |
| Ana-Exp | 24 | 20 | 0.20 | 6.20 |

it does not have the problems of 3D-FEM, such as being time-consuming and costly. The proposed method could be extended to calculate self- and mutual inductance for the computation of various chargers' coils, such as DD, DDQ, BP, QD, and extended DD, which are appropriate for DWC application.

## References


[1] S. Li and C. C. Mi, "Wireless power transfer for electric vehicle applications," *IEEE Journal of Emerging and Selected Topics in Power Electronics*, vol. 3, no. 1, pp. 4-17, 2014.

[2] B. H. Waters, A. P. Sample, P. Bonde, and J. R. Smith, "Powering a ventricular assist device (VAD) with the free-range resonant electrical energy delivery (FREE-D) system," *Proceedings of the IEEE*, vol. 100, no. 1, pp. 138-149, 2011.

[3] G. Scheible, J. Schutz, and C. Apneseth, "Novel wireless power supply system for wireless communication devices in industrial automation systems," in *Proceedings of IEEE 2002 28th Annual Conference of the Industrial Electronics Society*, Seville, Spain, 2002, pp. 1358-1363.

[4] R. C. Kuo, P. Riehl, A. Satyamoorthy, W. Plumb, P. Tustin, and J. Lin, "A 3D resonant wireless charger for a wearable device and a mobile phone," in *Proceedings of 2015 IEEE Wireless Power Transfer Conference (WPTC)*, Boulder, CO, 2015, pp. 1-3.

[5] A. A. Mohamed, A. A. Marim, and O. A. Mohammed, "Magnetic design considerations of bidirectional inductive wireless power transfer system for EV applications," *IEEE Transactions on Magnetics*, vol. 53, no. 6, pp. 1-5, 2017.

[6] W. Dehui, S. Qisheng, W. Xiaohong, and Y. Fan, "Analytical model of mutual coupling between rectangular spiral coils with lateral misalignment for wireless power applications," *IET Power Electronics*, vol. 11, no. 5, pp. 781-786, 2018.

[7] A. A. Mohamed, S. An, and O. Mohammed, "Coil design optimization of power pad in IPT system for electric vehicle applications," *IEEE Transactions on Magnetics*, vol. 54, no. 4, pp. 1-5, 2018.

[8] S. R. Khan, S. K. Pavuluri, and M. P. Desmulliez, "Accurate modeling of coil inductance for near-field wireless power transfer," *IEEE Transactions on Microwave Theory and Techniques*, vol. 66, no. 9, pp. 4158-4169, 2018.

[9] Z. H. Shi, X. Y. Chen, and Z. C. Qiu, "Modeling of mutual inductance between superconducting pancake coils used in wireless power transfer (WPT) systems," *IEEE Transactions on Applied Superconductivity*, vol. 29, no. 2, pp. 1-4, 2019.

[10] J. T. Conway, "Analytical solutions for the self-and mutual inductances of concentric coplanar disk coils," *IEEE Transactions on Magnetics*, vol. 49, no. 3, pp. 1135-1142, 2012.

[11] W. G. Hurley, M. C. Duffy, J. Zhang, I. Lope, B. Kunz, and W. H. Wolfle, "A unified approach to the calculation of self-and mutual-inductance for coaxial coils in air," *IEEE Transactions on Power Electronics*, vol. 30, no. 11, pp. 6155-6162, 2015.

[12] E. R. Joy, A. Dalal, and P. Kumar, "Accurate computation of mutual inductance of two air core square coils with lateral and angular misalignments in a flat planar surface," *IEEE Transactions on Magnetics*, vol. 50, no. 1, pp. 1-9, 2013.

[13] S. Raju, R. Wu, M. Chan, and C. P. Yue, "Modeling of mutual coupling between planar inductors in wireless power applications," *IEEE Transactions on Power Electronics*, vol. 29, no. 1, pp. 481-490, 2014.

[14] Z. Luo and X. Wei, "Analysis of square and circular planar spiral coils in wireless power transfer system for electric vehicles," *IEEE Transactions on Industrial Electronics*, vol. 65, no. 1, pp. 331-341, 2017.

[15] B. K. Kushwaha, G. Rituraj, and P. Kumar, "3-D analytical model for computation of mutual inductance for different misalignments with shielding in wireless power transfer system," *IEEE Transactions on Transportation Electrification*, vol. 3, no. 2, pp. 332-342, 2017.

[16] C. Peters and Y. Manoli, "Inductance calculation of planar multi-layer and multi-wire coils: an analytical approach," *Sensors and Actuators A: Physical*, vol. 145, pp. 394-404, 2008.

[17] H. K. Dashora, G. Buja, M. Bertoluzzo, R. Pinto, and V. Lopresto, "Analysis and design of DD coupler for dynamic wireless charging of electric vehicles," *Journal of Electromagnetic Waves and Applications*, vol. 32, no. 2, pp. 170-189, 2018.

[18] H. M. Greenhouse, "Design of planar rectangular microelectronic inductors," *IEEE Transactions on Parts, Hybrids, and Packaging*, vol. 10, no. 2, pp. 101-109, 1974.

[19] S. K. Burke, R. J. Ditchburn, and T. P. Theodoulidis, "Impedance of curved rectangular spiral coils around a conductive cylinder," *Journal of Applied Physics*, vol. 104, article no. 014912, 2008. https://doi.org/10.1063/1.2951947

[20] Y. Cheng and Y. Shu, "A new analytical calculation of the mutual inductance of the coaxial spiral rectangular coils," *IEEE Transactions on Magnetics*, vol. 50, no. 4, pp. 1-6, 2013.

[21] C. Peters and Y. Manoli, "Advanced telemetric powering of sensors using multi-wire coils," in *Proceedings of IEEE SENSORS*, Daegu, Korea, 2006, pp. 769-772.

[22] F. W. Grover, *Inductance Calculations: Working Formulas and Tables*. Mineola, NY: Dover Publications, 2004.

[23] H. Tavakkoli, E. Abbaspour-Sani, A. Khalilzadegan, G. Rezazadeh, and A. Khoei, "Analytical study of mutual inductance of hexagonal and octagonal spiral planer coils," *Sensors and Actuators A: Physical*, vol. 247, pp. 53-64, 2016.

[24] C. R. Paul, *Inductance: Loop and Partial*. Hoboken, NJ: John Wiley & Sons, 2011.

## Ali Alkasir

received an M.Sc. degree in electrical engineering, power electronic, and electrical machines from Babol Noshirvani University, Babol, Iran in 2019. His main research interests are the design and control of WPT systems and resonant converters. He is currently working as an R&D engineer at Khazar Transfo Corporation in the automation and design industrial rectifier fields.

## Seyedreza Abdollahi

received a Ph.D. in electronics engineering from Brunel University London, UK; MSc. degree from the University of Tehran; and BSc. degree from Isfahan University of Technology, Isfahan, I. R. of Iran. His research areas are focused on integrated wireless and optical communication circuits and systems. During his research at the Wireless Network Communication Centre at Brunel University London and the VLSI Lab at the University of Tehran, he presented and published the research outcomes at international conferences and in journal papers, one of which was registered as a patent. Currently, he is a faculty member of the ECE department at the University of Science and Technology of Mazandaran, where he is working on wireless and RF circuits and systems for RF energy harvesting and power transmission.

## Seyed Ehsan Abdollahi

received his B.Sc. degree from Amirkabir University of Technology, Tehran, Iran, in 2002; M.Sc. degree from Iran University of Science and Technology, Tehran, Iran, in 2005; and a Ph.D. from the University of Tehran, Iran, in 2014, all in electric power engineering. Currently he is an assistant professor electrical and computer engineering department of Babol Noshirvani University of Technology. His research interest is focused on electrical machines and transformer designs and modeling, power electronics, energy storage systems modeling and control.

## Patrick Wheeler

received his B.Eng. (Hons) degree in 1990 from the University of Bristol, UK. He received his Ph.D. in electrical engineering for his work on matrix converters from the University of Bristol, UK in 1994. In 1993, he moved to the University of Nottingham and worked as a research assistant in the Department of Electrical and Electronic Engineering. In 1996, he became a lecturer in the Power Electronics, Machines, and Control Group at the University of Nottingham, UK. Since January 2008, he has been a full professor in the same research group. He was head of the Department of Electrical and Electronic Engineering at the University of Nottingham from 2015 to 2018. He is currently the head of the Power Electronics, Machines, and Control Research Group, Global Director of the University of Nottingham's Institute of Aerospace Technology, and was the Li Dak Sum Chair Professor in Electrical and Aerospace Engineering. He is a member of the IEEE PELs AdCom and is currently IEEE PELS Vice President for Technical Operations. He has published over 750 academic publications in leading international conferences and journals.